Published OnlineFirst January 29, 2015; DOI: 10.1158/2326-6066.CIR-14-0165

IU/mL penicillin–streptomycin, 1.6 mmol/L L-glutamine, and 0.05 mmol/L β-mercaptoethanol (i.e., CM), after which they were bisected in a sterile environment and viable cells were scraped from the cutting surface. The SLN cells were washed twice in CM, counted, and further processed.

Cytokine profiling

Freshly isolated SLN cells were cultured overnight at 37°C (1×10^5 per 100 μL) in CM. The supernatants were harvested and stored at −20°C until detection of cytokine levels by BD-cytometric bead array (CBA; BD) following the manufacturer's instructions.

Flow cytometry

Freshly isolated SLN cells or thawed PBMCs were directly stained with antibodies labeled with either FITC, PE, PE-CY5.5, PerCP-CY5.5, or APC and analyzed by flow cytometry at 100,000 or 200,000 events per measurement, as previously described (25, 27). Monoclonal antibodies against CD1a, CD3, CD11c, CD14, CD16, CD19, CD25, CD40, CD56, CD80, CD86, CD123, CCR7, HLA-DR, CLEC9A, IgM, rIgG2a (BD), CD11c, CD40, CD83 (Immunotech), BDCA-1/CD1c, BDCA-2/CD303, BDCA-3/CD141 (Miltenyi Biotec), MDC-8 (kindly provided by Dr. E.P. Rieber, Institute for Immunology, Technical University of Dresden, Germany), and mIgM (Southern Biotechnology) with matching isotype control antibodies were used.

Quantitative real-time polymerase chain reaction

RNA (0.25 μg) was isolated from PBMCs and reverse transcribed into cDNA using a Revertaid H-minus cDNA synthesis kit (MBI Fermentas) according to the manufacturers' instructions and as described previously (28). Quantitative real-time PCR (qRT-PCR) was performed using an ABI Prism 7900HT Sequence detection system (Applied Biosystems) using SybrGreen (Applied Biosystems). Primers were designed using Primer Express software and guidelines (Applied Biosystems): *MxA* (*Genes Genbank accession no.* NM 002462): sense: TTCAGCACCTGATGGCCTATC, antisense: GTACGTCTGGAGCATGAAGAACTG; *GAPDH*: sense: GCCAGCCGAGCCACATC, antisense: TGACCAGGCGCCCAATAC. To calculate arbitrary values of mRNA levels and to correct for differences in primer efficiencies, a standard curve was constructed. Expression levels of *MxA* were expressed relative to the housekeeping gene *GAPDH*.

PBMC cultures

PBMCs from 4 healthy donors were cultured for 2 days at 5×10^6 cells/mL in CM at 37°C, without additives (neg. control), with 5 μg/mL CpG-A (ODN 2216), or with 5 μg/mL CpG-B (ODN 7909, PF-3512676; both from Coley Pharmaceutical Group), the latter either with or without 1,000 IU/mL GM-CSF (Leukine; Berlex Laboratories Inc.), at 1 mL/well/condition in a 48-well tissue culture plate. After 2 days, cells were harvested and analyzed by flow cytometry.

Cross-presentation assay

Cryostored SLN single-cell suspensions from HLA-A2$^+$ patients were thawed, washed in serum-free medium, and 1×10^5 SLN cells/50 μL/well were plated in 96-well round-bottom wells; triplicate wells were used for all below listed test conditions. To the wells, either no additives or a long (MART-1 aa16-40L) synthetic peptide (concentration 100 μg/mL) were added and the cells were left at 37°C for 2 hours, after which 50 μL of 20% FCS CM was added to each well and the cells were cultured overnight at 37°C in a humidified 5% CO_2 atmosphere. The following day, the cells were washed, and to the no-additive wells, either a short MART-1 aa26-35L or a short HIV RT aa476-484 (irrelevant) synthetic peptide were added at a concentration of 1 μg/mL in serum-free medium together with 3 μg/mL β2-microglobulin. After 2 hours of incubation at 37°C, all cells were washed and resuspended in 100 μL/well CM. Subsequently, 50,000 cells of a >90% pure MART-1 aa26-35L–specific CD8$^+$ T-cell bulk culture (determined by tetramer staining) were added in 100-μL CM per well, together with 0.5 μL of Golgi Plug (BD Biosciences), and incubated at 37°C in a humidified 5% CO_2 atmosphere for 5 hours. As a positive control, HLA-A2$^+$ JY stimulator cells loaded with MART-1 aa26-35L were also coincubated with the MART-specific HLA-A2–matched CD8$^+$ effector T cells. Subsequently, all cells were harvested, washed, stained for MART-1 aa26-35L HLA-A2-tetramer binding and intracellular (i.c.) IFNγ, and analyzed by flow cytometry as previously described (29).

Statistical analysis

Overall differences in patient or SLN characteristics and immune parameters were analyzed using the one-way ANOVA test. The *post hoc* multiple comparison Tukey test was used to analyze differences between two patient study groups. The paired samples *t* test was used to calculate differences in immune parameters between the PBMCs from the first and second time point. Correlations were determined using the Pearson *r* test. Differences were considered statistically significant when $P \leq 0.05$.

Results

Clinical observations

No statistically significant differences were found among the three patient groups receiving combined GM-CSF and PF-3512676 (hereafter referred to as CpG), CpG alone, or saline, in terms of age, gender, or Breslow Thickness (see Table 1A). Injections with CpG and/or GM-CSF were tolerated well. Common side effects were mild flu-like symptoms and induration at the injection site, all of which were transient and easily controlled by paracetamol. According to common toxicity criteria (NCI CTC Toxicity scale Version 2.0), 70% of patients receiving CpG and 56% of patients receiving GM-CSF/CpG had grade 1 fatigue and fever and/or grade 1 myalgia. Grade 2 injection site reactions were observed in 89% of patients receiving GM-CSF/CpG and in 50% of patients receiving CpG; grade 1 reactions were observed in 22% of patients receiving GM-CSF/CpG and in 30% of patients receiving CpG. Induration of the injection site remained present for 2 to 7 days after injection but was considered manageable by most patients. One patient's concern about the injection site induration led to the decision not to administer the second dose of GM-CSF and CpG but did not result in exclusion from the trial as the measured immune parameters in this patient did not deviate from others in the test group. No toxicity was observed in patients receiving saline. After pathologic examination, 5 SLNs were found to contain tumor cells, i.e., disease stage III. Four of these stage III patients had received saline, resulting in an uneven distribution over the three groups ($P = 0.031$, see Table 1A). The dissected SLNs of patients receiving GM-CSF/CpG were found larger in

Published OnlineFirst January 29, 2015; DOI: 10.1158/2326-6066.CIR-14-0165

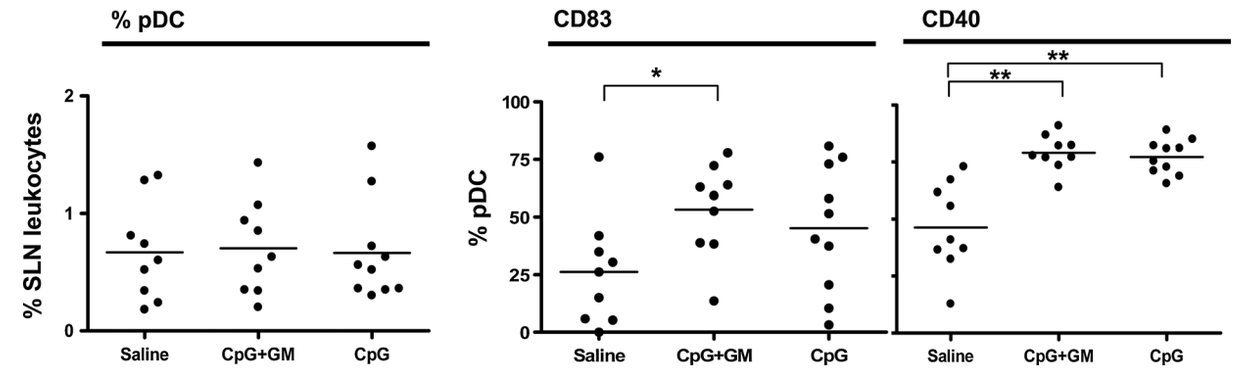

Figure 1.
Frequency and phenotype of pDCs in melanoma SLN. Shown are pDC frequencies (as percentage of SLN cells), CD83 and CD40 expression by percentage positivity of pDCs (scatter plots, means indicated), divided by patient group receiving either saline placebo, or 1 mg CpG-B and 100 μg GM-CSF (CpG+GM), or 1 mg CpG-B alone (CpG). Statistical significance: *, $P < 0.05$; **, $P < 0.01$.

comparison with the SLNs of the other groups ($P = 0.031$; see Table 1A). Also, cell yields were higher, but this did not reach statistical significance.

SLN cytokine release profiles

As an indication of innate immune activation, spontaneous cytokine release by SLN leukocytes was determined after 24-hour culture. As shown in Table 1B, compared with those of saline controls, the combined i.d. administration of GM-CSF and CpG resulted in the release of higher levels of the proinflammatory cytokines IL1β, IL6, and IL8; only the difference in the levels of IL6 reached statistical significance. This result is in keeping with reported CpG-induced IL6 release by pDCs (9) and consistent with an induced inflammatory environment in the SLN, which was enhanced by the addition of GM-CSF as evidenced by further elevated levels of IL1β, IL6, and IL8. Of note, we were unable to detect IFNα at this time point in any of the supernatants.

Effects on SLN DC subset composition

SLN cells, isolated on the day of operation, were analyzed by flow cytometry for the frequency and activation state of lymphocytic and DC subsets. No major shifts in overall lymphocyte subset

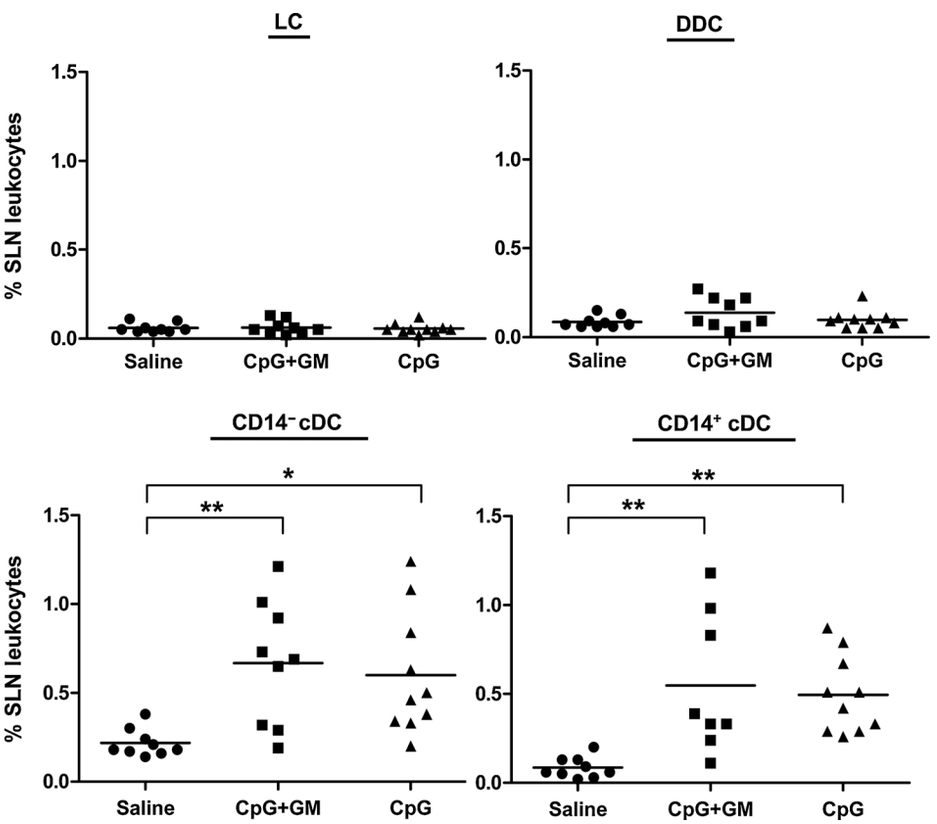

Figure 2.
Frequencies and phenotype of cDC subsets in melanoma SLN. Frequencies are shown as percentage of SLN cells, divided by patient group receiving either saline placebo, or 1 mg CpG-B and 100 μg GM-CSF (CpG+GM), or 1 mg CpG-B alone (CpG). The cDC subsets include LC, $CD1a^+$ DDCs, and $CD1a^-$ $CD14^-$ and $CD14^+$ LN-resident cDC subsets. Statistical significance: *, $P < 0.05$; **, $P < 0.01$.

Published OnlineFirst January 29, 2015; DOI: 10.1158/2326-6066.CIR-14-0165

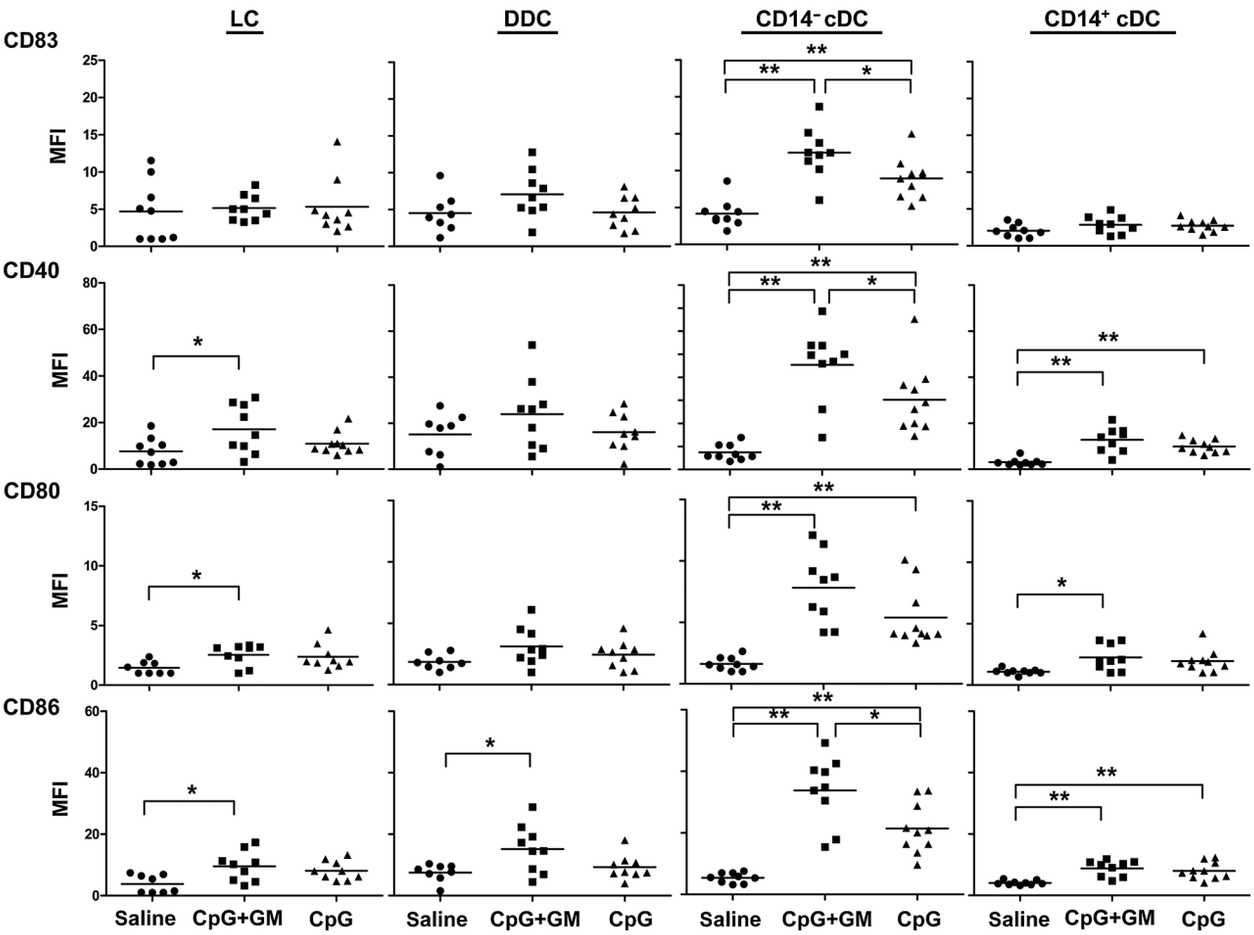

Figure 3.
Phenotype of cDC subsets in melanoma SLN. Expression levels of CD83 and costimulatory molecules of LC, CD1a$^+$ DDC, CD1a$^-$ CD14$^-$ and CD14$^+$ cDC subsets by mean fluorescence index (MFI) are shown. Means are indicated; patient groups received saline placebo, 1 mg CpG-B and 100 μg GM-CSF (CpG+GM), or 1 mg CpG-B alone (CpG). Statistical significance: *, $P < 0.05$; **, $P < 0.01$.

composition were observed between the test groups (data not shown). Although pDC rates were not elevated by administration of either GM-CSF/CpG or CpG alone, their activation state was, as evidenced by increased percentages of pDCs expressing the activation markers CD83 and CD40 (Fig. 1).

On the basis of CD1a, CD11c, and CD14 expression, four cDC subsets were discerned and phenotypically analyzed: (i) LC, (ii) DDC, (iii) CD14$^-$ cDC, and (iv) CD14$^+$ cDC, with the first two corresponding to skin-derived DCs (19, 30), and the latter two more likely representing LN-resident, blood-mobilized DC subsets (19). For gating strategies, we refer to Supplementary Fig. S1. Only the frequencies of both LN-resident cDC subsets were significantly upregulated in equal measure by either combined GM-CSF/CpG or CpG single administration (Fig. 2). These LN-resident subsets were further characterized in the steady state by relatively high expression levels of BDCA3 and, in particular for the CD14$^+$ cDCs, by CLEC9A (Supplementary Fig. S2), suggestive of their ability to take up necrotic cells and cross-present antigens to CTLs (23, 31, 32).

To assess cDC subset activation, expression levels of the maturation/costimulatory markers CD83, CD40, CD80, and CD86 were determined. As shown in Fig. 3, both CD1a$^-$ LN-resident cDC subsets, but the CD14$^-$ LN-resident subset in particular, displayed a stronger increase in activation state upon GM-CSF and/or CpG administration than the CD1a$^+$ skin-derived subsets. Whereas the CD14$^+$ cDCs were equally activated by combined GM-CSF/CpG or CpG alone, the CD14$^-$ subset was more activated by the combined regimen, with all activation markers consistently elevated to higher levels (Fig. 3).

Effects on DC (precursor) rates in peripheral blood: evidence for CpG + GM-CSF–induced activation and recruitment of BDCA3/CD141$^+$ cDC subsets

To ascertain systemic effects of low doses of locally administered CpG and GM-CSF, and to identify putative circulating precursors to the cDC subsets recruited to the SLN, frequencies and activation state of DC and monocytic subsets in PBMCs (27) were analyzed on the day of the first injection (day −7) and on the day of the SNP (day 0). Three cDC subsets were discerned in blood: cDC1 (BDCA1/CD1c$^+$), cDC2 (BDCA3/CD141$^+$), and cDC3 (M-DC8$^+$, also known as CD16$^+$CD14^{dim} or 6-Sulfo

Published OnlineFirst January 29, 2015; DOI: 10.1158/2326-6066.CIR-14-0165

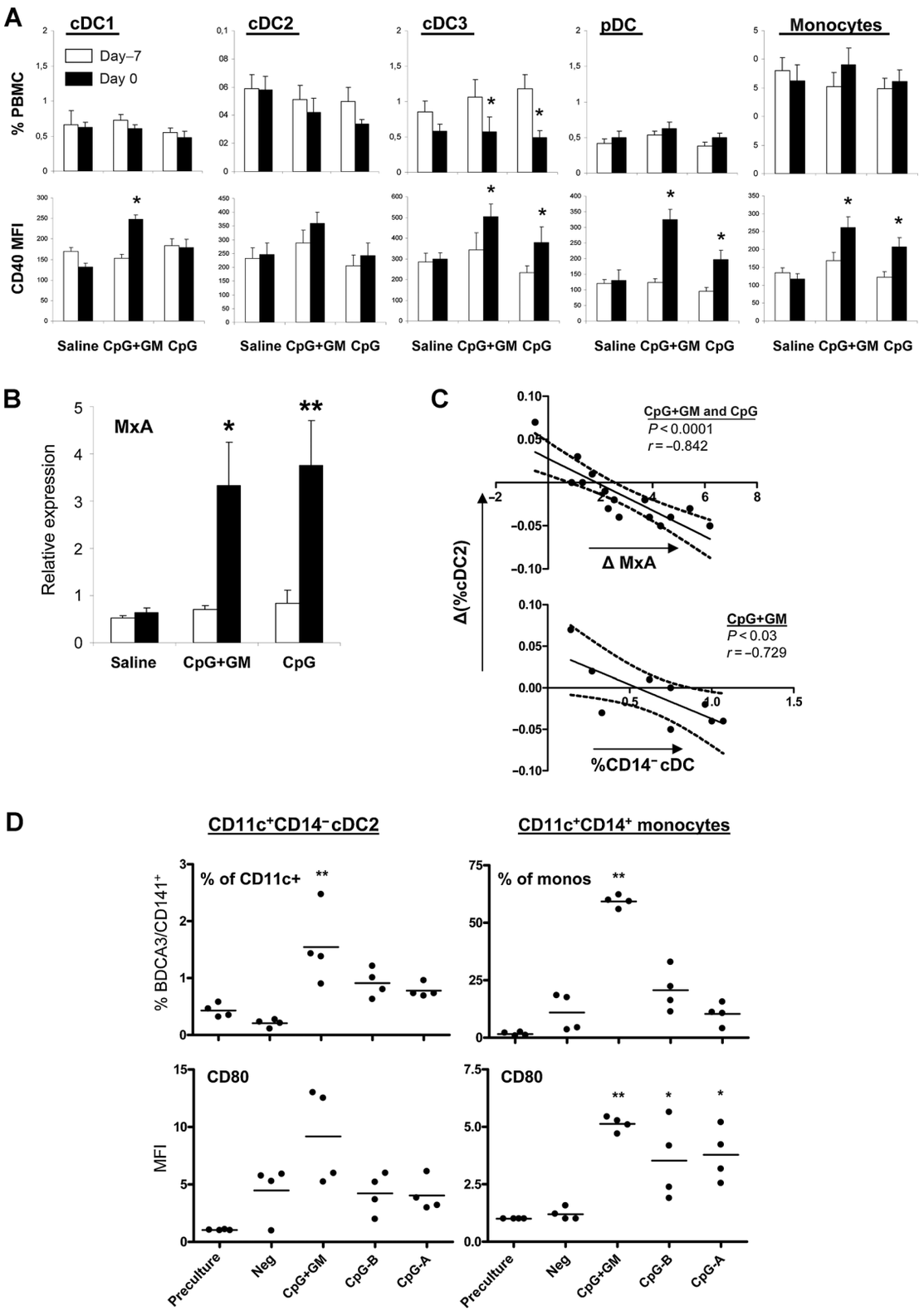

Published OnlineFirst January 29, 2015; DOI: 10.1158/2326-6066.CIR-14-0165

LacNac$^+$ (SLAN) inflammatory DCs (33). pDCs were defined as CD123$^+$BDCA2/CD303$^+$ and monocytes as CD11c^{hi}CD14$^+$. cDC2 and cDC3 frequencies were decreased upon either combined GM-CSF/CpG or single CpG administration, reaching statistical significance for cDC3 only (Fig. 4A). On the basis of CD40, CD86, and HLA-DR expression levels, combined i.d. GM-CSF/CpG delivery most profoundly affected myeloid maturation, with all APC subsets showing a measure of activation (shown for CD40 with statistical significance levels indicated in Fig. 4A). Of note, none of these subsets were activated by i.d. saline administration before SLN excision.

A likely mechanism of CpG-induced cDC recruitment to the SLN would be through IFNα-mediated activation of circulating cDC precursors, followed by their extravasation at inflammatory sites (e.g., CpG-conditioned skin or SLN). Although we were unable to detect IFNα either in supernatants of *ex vivo* cultured SLN suspensions or in plasma samples (data not shown), we did detect an increase in mRNA levels of the type I IFN-responsive gene product MxA by qRT-PCR in PBMC samples of the CpG-treated patient groups (Fig. 4B), clearly demonstrating a systemic impact of type I IFN release induced by locally administered CpG-B (most likely pDC-derived IFNα). Interestingly, CpG-related decreases of BDCA3/CD141$^+$ cDC2 frequencies in the blood directly and strongly correlated to ΔMxA transcript levels (Fig. 4C, top). Moreover, correlating frequencies of the four separate cDC subsets in SLNs and posttreatment changes in frequencies of the different cDC subsets and monocytes in peripheral blood, the only significant correlation found was between decreased cDC2 subset frequencies in the blood and higher BDCA3/CD141$^+$CD14$^-$ cDC rates in the SLNs of patients that received the combined administration of GM-CSF/CpG (Fig. 4C, bottom), but *not* of patients receiving CpG only (data not shown). This potential relationship was confirmed by the results of 2-day *in vitro* PBMC cultures, showing a significant increase and enhanced activation state (exemplified by CD80 expression) of BDCA3$^+$ cDC2 (and note: also of *de novo* BDCA3-expressing monocytes), upon culture with combined CpG-B and GM-CSF as compared with either CpG-B or CpG-A alone (Fig. 4D). CpG-A was taken along in these cultures as this class of ODN is known to induce higher release levels of type I IFN. Indeed, concentrations of IFNα in CpG-B–stimulated cultures averaged 27.6 pg/mL, while those in CpG-A–stimulated cultures exceeded 500 pg/mL. Nevertheless, the combined CpG-B/GM-CSF culture induced superior activation of both cDC2 and monocytes. These data are consistent with a CpG/type I IFN-related recruitment of BDCA3$^+$ cDC2 to the SLN, followed by their CpG/GM-CSF–induced maturation to BDCA3/CD141$^+$CD14$^-$ LN-resident cDCs.

Effects on cross-presentation in SLNs

As the observed expression of both BDCA3 and CLEC9A on the LN-resident cDC subsets in the steady state was suggestive of cross-presentation capacity, and as they were preferentially induced by CpG + GM-CSF, we compared the *ex vivo* (cross-) presentation ability of SLN suspensions among patients from all three treatment groups (Fig. 5A–C). Cryostored SLN suspensions of 3 HLA-A2$^+$ patients from each of the three treatment groups were available for this analysis. In line with the CpG + GM-CSF (CpG+GM)-induced activation and recruitment of putative cross-presenting BDCA3/CD141$^+$ cDC subsets to the SLN, it seemed that SLN cells from patients that received the combined administration of CpG+GM most efficiently cross-presented the immunodominant aa26-35L HLA-A2–binding epitope of MART-1 to a specific CD8$^+$ T-cell line after uptake and processing of a long 25-mer MART-1 (aa16-40L) peptide, whereas direct presentation of the aa25-35L short peptide was comparable among all three groups (Fig. 5B and C). Cross-presentation efficiency was determined by i.c. IFNγ expression in the MART-1 aa26-35L-specific T cells relative to the i.c. IFNγ level detected after presentation of the short peptide, to standardize between donors, samples, and assays. Unfortunately, statistical significance was not reached because of the low number of cryostored SLN samples available for this analysis (Fig. 5C). Of note, the observed increased cross-presentation capacity corresponded to predominant frequencies of CD1a$^-$ LN-resident subsets (with relatively high expression levels of BDCA3 and CLEC9A) and, accordingly, the observed cross-presentation efficiencies correlated with the sum-total rate of LN-resident CD1a$^-$ cDC subsets in the used SLN suspensions rather than with that of either CD1a$^+$ skin-migrated cDCs or pDCs (Fig. 5D).

Discussion

The results presented in this article are the first to show the effects of combined GM-CSF and CpG-B administration on human DC subsets in melanoma SLNs and the consequent outcome in terms of antigen cross-presentation. We previously showed that four daily i.d. injections of GM-CSF (at 3 μg/kg) increased the number and activation state of CD1a$^+$ cDCs in the SLNs (16) and presented evidence to suggest that these cells were contiguous with dermal CD1a$^+$CD83$^+$ DCs and had migrated

Figure 4.

Effects of CpG ± GM-CSF on the frequency and activation state of APC subsets in peripheral blood. A, frequency of various DC subsets and monocytes and expression levels of CD40 by mean fluorescence index (MFI). Patient groups are indicated: saline placebo, 1 mg CpG-B and 100 μg GM-CSF (CpG+GM), or 1 mg CpG-B alone (CpG). Open bars, day −7 (basal levels); closed bars, day 0, time of SLN excision. Statistical significance: *, $P < 0.05$; **, $P < 0.01$; mean ± SEM are shown. B, relative expression of transcripts from the type I IFN-responsive *mxa* gene, determined by reverse transcriptase quantitative PCR on PBMCs. Patient groups are indicated in the bar graphs: saline placebo, 1 mg CpG-B and 100 μg GM-CSF (CpG+GM), or 1 mg CpG-B alone (CpG). Open bars, day −7 (basal levels); closed bars, day 0, time of SLN excision. Statistical significance: *, $P < 0.05$ and **, $P < 0.01$. C, correlation between changes in BDCA3/CD141$^+$ peripheral blood cDC (cDC2) frequencies (between day −7 and 0) and corresponding MxA transcript levels in peripheral blood, and cDC2 frequencies and CD14$^-$ LN-resident cDC rates in the SLNs of patients who were administered 1 mg CpG-B and 100 μg GM-CSF (CpG+GM) at the primary melanoma excision site. Pearson r^2 and P values are listed and 95% confidentiality intervals indicated by dotted lines. D, frequencies of BDCA3/CD141$^+$ cDC2 (as % of gated CD11c$^+$ cells) and of BDCA3/CD141$^+$ monocytes (as % of CD14$^+$ monocytes) in PBMCs, before (preculture) and after 2 days of culture without additions (neg) or with added CpG-B and GM-CSF (CpG+GM), CpG-B, or CpG-A. Also shown are CD80 expression levels (in MFI) on the CC14$^-$BDCA3/CD141$^+$ cDC2 or monocytes. Asterisks denote statistically significant differences versus negative control cultures (neg): **, $P < 0.01$; *, $P < 0.05$. Note that MFI CD80 on CD11c$^+$CC14$^-$BDCA3/CD141$^+$ cDC2 were also significantly different between preculture and CpG+GM conditions ($P < 0.01$).

Published OnlineFirst January 29, 2015; DOI: 10.1158/2326-6066.CIR-14-0165

from the dermis, where GM-CSF was delivered at the primary melanoma excision site (30). In contrast, a single high dose of CpG-B (8 mg) did not result in increased rates of either the pDC or $CD1a^+$ cDC subsets, but increased the frequency of a $CD1a^-$ $CD11c^+CD83^+$ cDC subset (3). In the current trial, patients received two i.d. injections of lower doses of CpG-B alone (1 mg), or in combination with GM-CSF (100 μg). These doses were based on studies in which these compounds were added as adjuvants to i.d. applied vaccines (34, 35) and were chosen to minimize the chances of any side effects from their combined administration in early-stage melanoma patients participating in this trial.

Whereas in trials in which patients underwent multiple rounds of vaccination, suppressive effects were ascribed to the use of GM-CSF as vaccine adjuvant (34), limited low dosing as local immune stimulant was shown by us to lead to cDC maturation and concomitant antitumor T-cell activation (5, 16, 30). As anticipated, combined CpG/GM-CSF administration led to a more wide-ranging pDC and cDC subset activation than CpG alone, but it also led to the preferential recruitment of $BDCA3/CD141^+$ blood-derived cDC subsets, corresponding to the $CD1a^-CD11c^+CD83^+$ cDC population identified after CpG-B treatment in our previously reported trial (3), and which, in turn, we found to correlate with an increased functional *ex vivo* cross-presentation capacity of cells derived from the *in vivo* conditioned SLNs.

We previously identified two major $BDCA3/CD141^+$ SLN-resident cDC subsets, i.e., $CD1a^-CD14^-$ and $CD1a^-CD14^+$ cDCs (19). In the steady state (e.g., in saline-administered patients), $CD1a^-CD14^-$ cDCs express CD83 and costimulatory molecules at lower levels than the $CD1a^+$ skin-migratory cDC subsets (19). However, CpG and/or GM-CSF administration enhanced expression of these markers to levels exceeding those of $CD1a^+$ cDCs, demonstrating the great potential of this subset for T-cell activation under inflammatory conditions. Indeed, this is in keeping with our own previous findings showing that upon isolation from SLNs, this subset proved to be the most powerful T cell–stimulatory cDC subset, based on proliferation and induction of cytokine release (19). We found the frequencies of $CD1a^-CD14^-$ cDCs to be elevated in patients receiving CpG-B and to even higher levels in patients receiving combined CpG-B/GM-CSF. GM-CSF coadministration also further enhanced the CpG-induced maturation of this subset. Although CpG-B ODNs are generally poor IFNα inducers (11), increased MxA transcript levels in peripheral blood nevertheless demonstrated a systemic impact of the CpG-B-induced type I IFN release. Indeed, the $CD14^-$ cDC subset may be the *in vivo* equivalent of IFN-DCs generated *in vitro* in the presence of GM-CSF and IFNα (36). Like IFN-DCs, they have a dendritic morphology (19), are mature ($CD83^+$), and display high levels of costimulatory molecules; they express CCR7 (3), lack CD1a, but also express CD123 (19, 37). IFN-DCs express higher levels of MHC class I and associated antigen-processing elements than classical IL4-DCs (38, 39) and were shown to be superior Th1 and CTL inducers with low-level coactivation of Tregs (38–40). Moreover, they were reported to be optimally equipped for high-efficiency CTL cross-priming (41, 42). These phenotypic and functional characteristics strongly favor antitumor immunity.

Although $CD1a^-CD14^+$ cDCs morphologically resemble monocytic or macrophage-like cells, their CD83 expression (ranging from 12% to 95%) suggests a semimature DC phenotype (19). The observed increase in their frequencies upon local CpG-B administration is suggestive of their recruitment from blood-derived monocytes, most likely dependent on CpG-induced type I IFN. Monocytes express extremely low levels of TLR9 transcripts, and their *in vitro* activation by CpG requires the presence of pDCs, a rich source of IFNα (43). IFNα-activated monocytes acquire a $CD14^+CD123^+CD83^+$ phenotype but maintain a monocytic appearance, reminiscent of the $CD14^+$ cDC subset in SLNs (19), and have been shown to stimulate memory T cells (44). This may be relevant to their activity in SLNs, where previously primed antimelanoma T cells are present and "poised" for reactivation (4, 5).

Locally administered CpG and GM-CSF also affected the *in vivo* activation state of DC subsets in peripheral blood. The exact relationship between DC subsets and SLN subsets may not be simply deduced by phenotypic similarities and correlation between frequencies in blood and SLNs, because of their phenotypic plasticity and possible simultaneous recruitment to the periphery and mobilization from the bone marrow. It nevertheless seems plausible that the activated $M\text{-}DC8^+$ SLAN-cDC subset (significantly reduced in posttreatment blood) was recruited to the site of CpG administration, because this subset has been associated with rapid migration to sites of inflammation (33). Most notably, a significant correlation between decreased $BDCA3/CD141^+$ cDC2 rates in peripheral blood and increased $CD1a^-CD14^-$ cDC frequencies in the SLNs of patients receiving combined CpG/GM-CSF, suggests cDC2 to be the precursors of the $BDCA3^+$ $CD1a^-CD14^-$ SLN-resident cDC subset. Indeed, this was suggested by our *in vitro* observation that cDC2 frequencies and their maturation state both increased significantly upon culture in the presence of CpG combined with GM-CSF. Results from the same experiments also identified monocytes as possible precursors of the $BDCA3/CD141^+$ $CD14^+$ cDC subset, as they acquired both BDCA3/CD141 and CD80 expression upon 48 hours exposure to CpG ± GM-CSF.

We showed both $CD1a^-$ LN-resident cDC subsets to express BDCA3/CD141 (also known as thrombomodulin) and CLEC9A in the steady state (i.e., in untreated SLN samples). Intriguingly, genome-wide transcriptional profiling pointed to $BDCA3^+$ DCs as the human equivalent of the $CD8\alpha^+$ DC subset in the murine spleen, which is known to be the subset with powerful CTL cross-priming ability (45), an important feature for the generation of antitumor immunity. *In vitro* studies demonstrated the ability of human $BDCA3^+$ DCs to cross-prime CTLs and thus confirmed this hypothesis (23, 31, 32). CLEC9A, a C-type Lectin receptor was recently shown to be preferentially expressed on $BDCA3^+$ cDCs (32) in the blood and to bind extracellularly exposed actin, thus facilitating cross-priming from necrotic cell-derived proteins (46). We found CLEC9A expressed to varying extent on all cDC subsets in the SLNs but in particularly high levels on the $CD14^+$ cDC subset that also expressed relatively high levels of BDCA3. Our finding of selective *in vivo* recruitment of $BDCA3^+$ cDC subsets to the SLNs that can also express CLEC9A, a corresponding enhanced *ex vivo* cross-presenting ability of *in vivo* CpG+GM-CSF–exposed SLN cells, and the *in vitro* maturation and induction of BDCA3 expression of both cDC2 and monocytes by CpG-B and GM-CSF, thus attests to the utility of this combination as an adjuvant for protein or long peptide vaccines that require cross-priming. This was confirmed

Published OnlineFirst January 29, 2015; DOI: 10.1158/2326-6066.CIR-14-0165

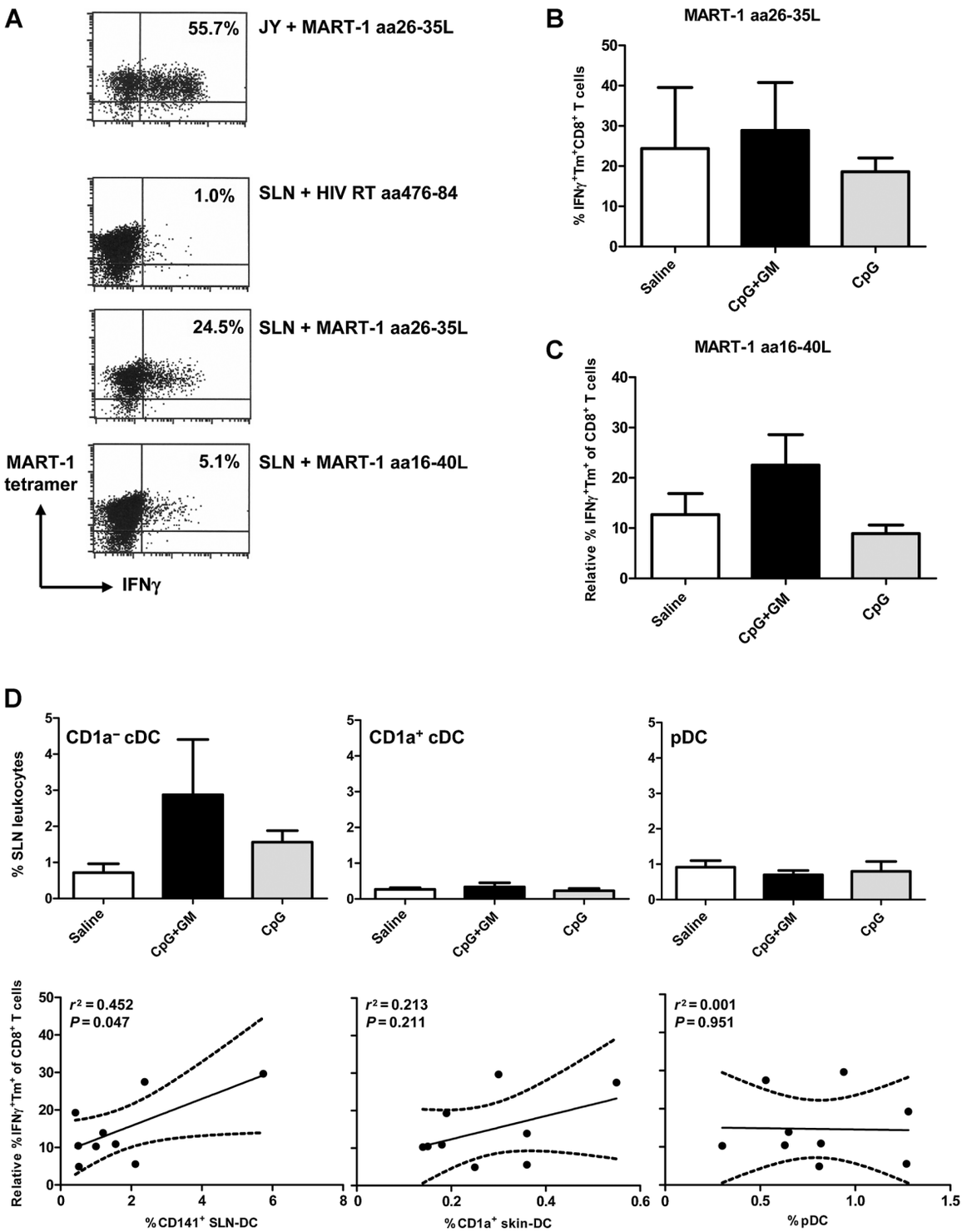

Figure 5.

Increased cross-presenting capacity of SLN single-cell suspensions from patients who received local CpG-B and GM-CSF. A, representative plots of intracellular (i.c.) IFNγ production by >90% pure HLA-A2–matched MART-1 aa26-35L–specific $CD8^+$ bulk T cells after incubation with respectively (from top to bottom): MART-1 aa26-35L (short peptide)–loaded JY cells, HIV RT aa476-484 (short-peptide)–loaded SLN cells, MART-1 aa26-35L (short peptide)–loaded SLN cells and MART-1 aa16-40L (long peptide)–loaded SLN cells. SLN single-cell suspension was from a CpG+GM-treated patient. B, average (±SEM) i.c. IFNγ-positive MART-1 aa26-35L–specific $CD8^+$ T cells after incubation with MART-1 aa26-35L (short peptide)–loaded and HLA-A2–matched SLN cells; Tm, tetramer. C, average (±SEM) i.c. IFNγ-positive MART-1 aa26-35L–specific $CD8^+$ T cells after incubation with MART-1 aa16-40L (long peptide)–loaded SLN cells (relative to i.c. IFNγ expression after incubation with the short peptide). Results shown are from SLN single-cell suspensions derived from HLA-$A2^+$ patients from the three indicated groups ($n = 3$ per group). D, percentages of $CD1a^-$ skin-resident cDC subsets, $CD1a^+$ skin-migrated cDC subsets, and pDCs in each of the three indicated patient groups tested for SLN cross-presenting ability (top; $n = 3$ per group) and correlation between the measured MART-1 aa16-40L cross-presenting efficiencies and frequencies of the respective $CD1a^-$ or $CD1a^+$ cDC subsets and the pDC subset (bottom). Pearson r^2 and P values are listed and 95% confidentiality intervals indicated by dotted lines.

Published OnlineFirst January 29, 2015; DOI: 10.1158/2326-6066.CIR-14-0165

in vivo, showing superior cross-priming by splenic CD8α after CpG stimulation, leading to tumor rejection (15, 47); remarkably, GM-CSF synergized with CpG to optimize this effect (47). Recently, $CD1a^+/CD1c^+$ as well as $BDCA3/CD141^+$ cDC subsets from LNs and tonsils were shown to have cross-presenting abilities (20, 48). Although the small numbers of viable SLN cells that we obtained from our treated patients prohibited DC subset sorting, we found the *ex vivo* cross-presenting ability of SLN cells of a MART-1–derived synthetic long peptide to correlate with frequencies of $CD1a^-BDCA3/CD141^+$ cDCs rather than of $CD1a^+$ skin-derived cDCs or pDCs, indicating that the $CD1a^-CD141^+/BDCA3^+$ LN-resident cDC subsets in particular may contribute to CTL-mediated immunity against melanoma antigens afforded by combined local administration of CpG-B and GM-CSF.

In conclusion, cross-talk between pDCs and cDCs has been shown to enhance their mutual activation and to benefit the generation of cell-mediated immunity (10, 15, 49, 50). As such, concerted activation and recruitment of pDC and $BDCA3/CD141^+$ cDC subsets, achieved by local delivery of combined CpG-B and GM-CSF, may greatly enhance antitumor immunity and support immunotherapy or other conventional therapies that induce the release of (necrotic cell-associated) tumor antigens and thus facilitate cross-priming of antitumor CTLs. The resulting immunity may afford a level of protection against (distant) recurrences. Indeed, preliminary follow-up analyses of patients participating in this study point to prolonged recurrence-free survival of the intervention groups (B.D. Koster and colleagues, manuscript in preparation). If this observation holds up in more extensive analyses and larger follow-up trials, this simple and generally applicable approach of local immune potentiation may provide an effective adjuvant therapy option for patients with early-stage melanoma.

Disclosure of Potential Conflicts of Interest

No potential conflicts of interest were disclosed.

Authors' Contributions

Conception and design: P.A.M. van Leeuwen, M.P. van den Tol, A.J.M. van den Eertwegh, R.J. Scheper, T.D. de Gruijl

Development of methodology: P.A.M. van Leeuwen, C.L. Verweij, R.J. Scheper

Acquisition of data (provided animals, acquired and managed patients, provided facilities, etc.): B.J.R. Sluijter, M.F.C.M. van den Hout, B.D. Koster, P.A.M. van Leeuwen, F.L. Schneiders, B.G. Molenkamp, S. Vosslamber, M.P. van den Tol, A.J.M. van den Eertwegh

Analysis and interpretation of data (e.g., statistical analysis, biostatistics, computational analysis): B.J.R. Sluijter, M.F.C.M. van den Hout, B.D. Koster, P.A.M. van Leeuwen, R. van de Ven, B.G. Molenkamp, S. Vosslamber, C.L. Verweij, A.J.M. van den Eertwegh, T.D. de Gruijl

Writing, review, and/or revision of the manuscript: B.J.R. Sluijter, M.F.C.M. van den Hout, P.A.M. van Leeuwen, F.L. Schneiders, R. van de Ven, M.P. van den Tol, A.J.M. van den Eertwegh, T.D. de Gruijl

Administrative, technical, or material support (i.e., reporting or organizing data, constructing databases): M.F.C.M. van den Hout, B.D. Koster

Study supervision: P.A.M. van Leeuwen, M.P. van den Tol, A.J.M. van den Eertwegh, T.D. de Gruijl

Acknowledgments

The authors thank Sinéad Lougheed for excellent technical assistance.

Grant Support

This work was supported, in part, by the Netherlands Organization for Scientific Research, NWO VIDI grant 917-56-321 to T.D. de Gruijl.

The costs of publication of this article were defrayed in part by the payment of page charges. This article must therefore be hereby marked *advertisement* in accordance with 18 U.S.C. Section 1734 solely to indicate this fact.

Received September 4, 2014; revised January 9, 2015; accepted January 22, 2015; published OnlineFirst January 29, 2015.

References

1. Cochran AJ, Morton DL, Stern S, Lana AM, Essner R, Wen DR. Sentinel lymph nodes show profound downregulation of antigen-presenting cells of the paracortex: implications for tumor biology and treatment. Mod Pathol 2001;14:604–8.
2. Lee JH, Torisu-Itakara H, Cochran AJ, Kadison A, Huynh Y, Morton DL, et al. Quantitative analysis of melanoma-induced cytokine-mediated immunosuppression in melanoma sentinel nodes. Clin Cancer Res 2005; 11:107–12.
3. Molenkamp BG, van Leeuwen PA, Meijer S, Sluijter BJ, Wijnands PG, Baars A, et al. Intradermal CpG-B activates both plasmacytoid and myeloid dendritic cells in the sentinel lymph node of melanoma patients. Clin Cancer Res 2007;13:2961–9.
4. Molenkamp BG, Sluijter BJ, van Leeuwen PA, Meijer S, Wijnands PG, van den Eertwegh AJ, et al. Local administration of PF-3512676 CpG-B instigates tumor-specific $CD8^+$ T cell reactivity in melanoma patients. Clin Cancer Res 2008;14:4532–42.
5. Vuylsteke RJ, Molenkamp BG, van Leeuwen PA, Meijer S, Wijnands PG, Haanen JB, et al. Tumor-specific $CD8^+$ T cell reactivity in the sentinel lymph node of GM-CSF-treated stage I melanoma patients is associated with high myeloid dendritic cell content. Clin Cancer Res 2006;12: 2826–33.
6. Wang W, Edington HD, Rao UNM, Jukic DM, Radfar A, Wang H, et al. Effects of high-dose IFN alpha 2b on regional lymph node metastases of human melanoma: modulation of STAT5, FOXP3, and IL-17. Clin Cancer Res 2008;14:8314–20.
7. Brody JD, Ai WZ, Czerwinski DK, Torchia JA, Levy M, Advani RH, et al. *In situ* vaccination with a TLR9 agonist induces systemic lymphoma regression: a phase I/II study. J Clin Oncol 2010;28:4324–32.
8. Kim YH, Gratzinger D, Harrison C, Brody JD, Czerwinski DK, Ai WZ, et al. *In situ* vaccination against mycosis fungoides by intratumoral injection of a TLR9 agonist combined with radiation: a phase 1/2 study. Blood 2012; 119:355–63.
9. Tel J, Lambeck AJ, Cruz LJ, Tacken PJ, de Vries IJ, Figdor CG. Human plasmacytoid dendritic cells phagocytose, process, and present exogenous particulate antigen. J Immunol 2010;184:4276–83.
10. Lou Y, Liu C, Kim GJ, Liu YJ, Hwu P, Wang G. Plasmacytoid dendritic cells synergize with myeloid dendritic cells in the induction of antigen-specific antitumor immune responses. J Immunol 2007;178:1534–41.
11. Vollmer J, Krieg AM. Immunotherapeutic applications of CpG oligodeoxynucleotide TLR9 agonists. Adv Drug Deliv Rev 2009;61:195–204.
12. Patterson S. Flexibility and cooperation among dendritic cells. Nat Immunol 2000;1:273–4.
13. Kawarada Y, Ganss R, Garbi N, Sacher T, Arnold B, Hammerling GJ. NK- and CD8(+) T cell-mediated eradication of established tumors by peritumoral injection of CpG-containing oligodeoxynucleotides. J Immunol 2001;167:5247–53.
14. Gursel M, Verthelyi D, Klinman DM. CpG oligodeoxynucleotides induce human monocytes to mature into functional dendritic cells. Eur J Immunol 2002;32:2617–22.
15. Nierkens S, den Brok MH, Garcia Z, Togher S, Wagenaars J, Wassink M, et al. Immune adjuvant efficacy of CpG oligonucleotide in cancer treatment is founded specifically upon TLR9 function in plasmacytoid dendritic cells. Cancer Res 2011;71:6428–37.
16. Vuylsteke RJCLM, Molenkamp BG, Gietema HA, van Leeuwen PAM, Wijnands PGJTB, Vos W, et al. Local administration of granulocyte/macrophage colony-stimulating factor increases the number and activation

Published OnlineFirst January 29, 2015; DOI: 10.1158/2326-6066.CIR-14-0165

state of dendritic cells in the sentinel lymph node of early-stage melanoma. Cancer Res 2004;64:8456–60.
17. Sandler AD, Chihara H, Kobayashi G, Zhu X, Miller MA, Scott DL, et al. CpG oligonucleotides enhance the tumor antigen-specific immune response of a granulocyte macrophage colony-stimulating factor-based vaccine strategy in neuroblastoma. Cancer Res 2003;63:394–9.
18. Tarhini AA, Leng SY, Moschos SJ, Yin Y, Sander C, Lin Y, et al. Safety and immunogenicity of vaccination with MART-1 (26-35, 27L), gp100 (209-217, 210M), and tyrosinase (368-376, 370D) in adjuvant with PF-3512676 and GM-CSF in metastatic melanoma. J Immunother 2012;35:359–66.
19. van de Ven R, van den Hout MF, Lindenberg JJ, Sluijter BJ, van Leeuwen PA, Lougheed SM, et al. Characterization of four conventional dendritic cell subsets in human skin-draining lymph nodes in relation to T-cell activation. Blood 2011;118:2502–10.
20. Segura E, Valladeau-Guilemond J, Donnadieu MH, Sastre-Garau X, Soumelis V, Amigorena S. Characterization of resident and migratory dendritic cells in human lymph nodes. J Exp Med 2012;209:653–60.
21. Nestle FO, Nickoloff BJ. Deepening our understanding of immune sentinels in the skin. J Clin Invest 2007;117:2382–5.
22. Santegoets SJAM, Bontkes HJ, Stam AGM, Bhoelan F, Ruizendaal JJ, van den Eertwegh AJM, et al. Inducing antitumor T cell immunity: comparative functional analysis of interstitial versus Langerhans dendritic cells in a human cell line model. J Immunol 2008;180:4540–9.
23. Bachem A, Guttler S, Hartung E, Ebstein F, Schaefer M, Tannert A, et al. Superior antigen cross-presentation and XCR1 expression define human $CD11c^{+}CD141^{+}$ cells as homologues of mouse $CD8^{+}$ dendritic cells. J Exp Med 2010;207:1273–81.
24. Veen Hvd, Hoekstra OS, Paul MA, Cuesta MA, Meijer S. Gamma probe-guided sentinel node biopsy to select patients with melanoma for lymphadenectomy. Br J Surg 1994;81:1769–70.
25. Vuylsteke RJCLM, van Leeuwen PAM, Meijer S, Wijnands PGJTB, Statius Muller MG, Busch DH, et al. Sampling tumor-draining lymph nodes for phenotypic and functional analysis of dendritic cells and T cells. Am J Pathol 2002;161:19–26.
26. Elliott B, Cook MG, John RJ, Powell BW, Pandha H, Dalgleish AG. Successful live cell harvest from bisected sentinel lymph nodes research report. J Immunol Methods 2004;291:71–8.
27. van CH, van der Veldt AA, Vroling L, Oosterhoff D, Broxterman HJ, Scheper RJ, et al. Sunitinib-induced myeloid lineage redistribution in renal cell cancer patients: $CD1c^{+}$ dendritic cell frequency predicts progression-free survival. Clin Cancer Res 2008;14:5884–92.
28. van Baarsen LG, Wijbrandts CA, Rustenburg F, Cantaert T, van der Pouw Kraan TC, Baeten DL, et al. Regulation of IFN response gene activity during infliximab treatment in rheumatoid arthritis is associated with clinical response to treatment. Arthritis Res Ther 2010;12:R11.
29. Schneiders FL, de Bruin RCG, Santegoets SJAM, Bonneville M, Scotet E, Scheper RJ, et al. Activated iNKT cells promote V gamma 9V delta 2-T cell anti-tumor effector functions through the production of TNF-alpha. Clin Immunol 2012;142:194–200.
30. Molenkamp BG, Vuylsteke RJ, van Leeuwen PA, Meijer S, Vos W, Wijnands PG, et al. Matched skin and sentinel lymph node samples of melanoma patients reveal exclusive migration of mature dendritic cells. Am J Pathol 2005;167:1301–7.
31. Jongbloed SL, Kassianos AJ, McDonald KJ, Clark GJ, Ju X, Angel CE, et al. Human $CD141^{+}$ $(BDCA\text{-}3)^{+}$ dendritic cells (DCs) represent a unique myeloid DC subset that cross-presents necrotic cell antigens. J Exp Med 2010;207:1247–60.
32. Poulin LF, Salio M, Griessinger E, njos-Afonso F, Craciun L, Chen JL, et al. Characterization of human $DNGR\text{-}1^{+}$ $BDCA3^{+}$ leukocytes as putative equivalents of mouse $CD8alpha^{+}$ dendritic cells. J Exp Med 2010;207:1261–71.
33. Schakel K, von KM, Hansel A, Ebling A, Schulze L, Haase M, et al. Human 6-sulfo LacNAc-expressing dendritic cells are principal producers of early interleukin-12 and are controlled by erythrocytes. Immunity 2006;24:767–77.
34. Clive KS, Tyler JA, Clifton GT, Holmes JP, Mittendorf EA, Ponniah S, et al. Use of GM-CSF as an adjuvant with cancer vaccines: beneficial or detrimental? Expert Rev Vaccines 2010;9:519–25.
35. Speiser DE, Lienard D, Rufer N, Rubio-Godoy V, Rimoldi D, Lejeune F, et al. Rapid and strong human CD8(+) T cell responses to vaccination with peptide, IFA, and CpG oligodeoxynucleotide 7909. J Clin Invest 2005;115:739–46.
36. Hartmann G, Weiner GJ, Krieg AM. CpG DNA: a potent signal for growth, activation, and maturation of human dendritic cells. Proc Natl Acad Sci U S A 1999;96:9305–10.
37. la Bella S, Nicola S, Riva A, Biasin M, Clerici M, Villa ML. Functional repertoire of dendritic cells generated in granulocyte macrophage-colony stimulating factor and interferon-alpha. J Leukoc Biol 2004;75:106–16.
38. Tosello V, Zamarchi R, Merlo A, Gorza M, Piovan E, Mandruzzato S, et al. Differential expression of constitutive and inducible proteasome subunits in human monocyte-derived DC differentiated in the presence of IFN-alpha or IL-4. Eur J Immunol 2009;39:56–66.
39. Mohty M, Vialle-Castellano A, Nunes JA, Isnardon D, Olive D, Gaugler B. IFN-alpha skews monocyte differentiation into Toll-like receptor 7-expressing dendritic cells with potent functional activities. J Immunol 2003;171:3385–93.
40. Gigante M, Mandic M, Wesa AK, Cavalcanti E, Dambrosio M, Mancini V, et al. Interferon-alpha (IFN-alpha)-conditioned DC preferentially stimulate type-1 and limit Treg-type *in vitro* T-cell responses from RCC patients. J Immunother 2008;31:254–62.
41. Lapenta C, Santini SM, Spada M, Donati S, Urbani F, Accapezzato D, et al. IFN-alpha-conditioned dendritic cells are highly efficient in inducing cross-priming CD8(+) T cells against exogenous viral antigens. Eur J Immunol 2006;36:2046–60.
42. Spadaro F, Lapenta C, Donati S, Abalsamo L, Barnaba V, Belardelli F, et al. IFN-alpha enhances cross-presentation in human dendritic cells by modulating antigen survival, endocytic routing, and processing. Blood 2012;119:1407–17.
43. Hornung V, Rothenfusser S, Britsch S, Krug A, Jahrsdorfer B, Giese T, et al. Quantitative expression of toll-like receptor 1-10 mRNA in cellular subsets of human peripheral blood mononuclear cells and sensitivity to CpG oligodeoxynucleotides. J Immunol 2002;168:4531–7.
44. Gerlini G, Mariotti G, Chiarugi A, Di GP, Caporale R, Parenti A, et al. Induction of $CD83^{+}CD14^{+}$ nondendritic antigen-presenting cells by exposure of monocytes to IFN-alpha. J Immunol 2008;181:2999–3008.
45. Robbins SH, Walzer T, Dembele D, Thibault C, Defays A, Bessou G, et al. Novel insights into the relationships between dendritic cell subsets in human and mouse revealed by genome-wide expression profiling. Genome Biol 2008;9:R17.
46. Ahrens S, Zelenay S, Sancho D, Hanc P, Kjaer S, Feest C, et al. F-actin is an evolutionarily conserved damage-associated molecular pattern recognized by DNGR-1, a receptor for dead cells. Immunity 2012;36:635–45.
47. de Brito C, Tomkowiak M, Ghittoni R, Caux C, Leverrier Y, Marvel J. CpG promotes cross-presentation of dead cell-associated antigens by pre-CD8 alpha(+) dendritic dells. J Immunol 2011;186:1503–11.
48. Segura E, Durand M, Amigorena S. Similar antigen cross-presentation capacity and phagocytic functions in all freshly isolated human lymphoid organ-resident dendritic cells. J Exp Med 2013;210:1035–47.
49. Kuwajima S, Sato T, Ishida K, Tada H, Tezuka H, Ohteki T. Interleukin 15-dependent crosstalk between conventional and plasmacytoid dendritic cells is essential for CpG-induced immune activation. Nat Immunol 2006;7:740–6.
50. Piccioli D, Tavarini S, Borgogni E, Steri V, Nuti S, Sammicheli C, et al. Functional specialization of human circulating CD16 and CD1c myeloid dendritic-cell subsets. Blood 2007;109:5371–9.